Preservation of Passivity During RLC Network Reduction via Split Congruence Transformations

Kevin J. Kerns and Andrew T. Yang

Department of Electrical Engineering
University of Washington

None of the existing network reduction tools preserve passivity for RLC networks. The loss of passivity can be a serious problem because simulations of the reduced networks may encounter "time step too small" errors. This paper presents a set of transformations called "Split Congruence Transformations" (SCT's) which can be used to accurately reduce a RLC network while preserving passivity.

1. Introduction

VLSI circuits are being designed to run faster and to use less power. To do this, designs are more aggressive, device sizes are shrinking, and power supplies are lower voltage. These trends cause layout-dependent and package-dependent parasitic effects to become more important. As result, simulations of a circuit must include models of the on-chip and off-chip parasitics in order to verify functionality before fabrication, and these models are often formed from lumped RLC networks [1][2][3]. Unfortunately, these models are usually so large that subsequent simulation become impractical or impossible, and the networks must be reduced before simulation.

None of the reduction algorithms which currently exist preserve passivity for general RLC networks. Passivity implies that a network cannot generate more energy than it absorbs, and no passive termination of the network will cause the system to be unstable. A passive network is asymptotically stable (i.e. the real parts of the poles are less than or equal to zero), but asymptotic stability does not imply passivity.

This paper presents a set of transformations called "Split Congruence Transformations" (SCT's) which can be used to reduce RLC networks accurately while preserving passivity. The reduced network is formulated in admittance parameters so that it can be directly added to the non-RLC elements of the original circuit for simulation.

The simplest algorithm which can be used for RLC network reduction is called "Asymptotic Waveform Evaluation" (AWE) [4]. The multiport admittance is approximated in the Laplace domain with a Taylor series, and a rational polynomial is derived via the Padé approximation which has the same moments as the series. This technique is ill conditioned so that matching more moments does not imply better accuracy. An extension to AWE, called "Complex Frequency Hopping" (CFH) [5], circumvents this problem by carrying out the Taylor series expansion at multiple locations on the imaginary axis. It is not a Padé approximation since it preserves poles rather than moments.

Krylov subspace techniques, which include the Lanczos and Arnoldi processes, can be used to formulate networks in a well conditioned manner by implicitly matching moments. A Krylov subspace of the matrix $\mathbf{A}$ and the column vectors contained in $\mathbf{V}$ is defined as

$$\mathbf{K}_q(\mathbf{A}, \mathbf{V}) = \text{span}\{\mathbf{V}, \mathbf{AV}, \ldots, \mathbf{A}^{q-1}\mathbf{V}\}\ . \tag{1}$$

A general multiport network reduction algorithm called "Matrix Padé via a Lanczos-type Process" (MPVL) uses the Lanczos process to match two moments per m internal nodes where m is the number of ports [6]. A similar technique, which is not a Padé approximation and is based on Arnoldi's method, was also presented for the reduction of RL networks [7], but it is easily extensible to general RLC networks.

None of the methods reviewed here preserve passivity, and only CFH preserves asymptotic stability. The other techniques can achieve asymptotic stability by post processing to eliminate unstable poles, but passivity is not easily ensured. *Even if asymptotic stability is preserved, a nonpassive reduced network in a circuit can create instabilities which cause the circuit simulation to fail.*

The purpose of this paper is not to present a specific reduction process or tool. Rather, the intent is to present a class of transformations that can be used to form different types of well conditioned RLC network reduction tools which preserve passivity. To this end, Section 2 presents conditions sufficient for passivity called the "passive form," and Section 3 provides a class of transformations called "Split Congruence Transformations" (SCT's) preserve the passive form and thus passivity. Section 4 shows SCT's which can be used to reduce a network while preserving admittance moments or poles, and Section 5 contains examples which demonstrate the reduction of RLC networks. Concluding remarks are made in Section 6.

2. The Passive Form of an RLC Network

In this section, it is shown that RLC network matrices formed using Modified Nodal Analysis (MNA) [9] have a special form, called the "passive form," which provide conditions sufficient for passivity. MNA can be used to formulate symmetric matrices which relate network voltages and currents to the inputs in the frequency domain as

$$(\mathbf{G} + s\mathbf{C})\,\mathbf{x} = \mathbf{b}\ . \tag{2}$$

Here the time independent elements are represented by $\mathbf{G}$ and the time dependent elements are represented by $\mathbf{C}$. MNA uses two types of variables to represent the state of the network — type 1 and type 2 state variables are nodal voltages and branch currents respectively. Corresponding to this definition, type 1 branch elements are those which can be represented as admittances such as nonzero resistors (conductors) and capacitors. Type 2 elements are those which can be represented as impedances such as resistors and inductors. Each type 2 element requires one state variable to represent branch current, and, as a result, resistors are usually stamped as type 1 in order to minimize the number of unknowns.

Equation (2) is partitioned into type 1 and type 2 components,

$$\left(\begin{bmatrix} \mathbf{G}_1 & \mathbf{G}_3^{\mathbf{T}} \\ \mathbf{G}_3 & \mathbf{G}_2 \end{bmatrix} + s\begin{bmatrix} \mathbf{C}_1 & \mathbf{0} \\ \mathbf{0} & \mathbf{C}_2 \end{bmatrix}\right)\begin{bmatrix} \mathbf{x}_1 \\ \mathbf{x}_2 \end{bmatrix} = \begin{bmatrix} \mathbf{b}_1 \\ \mathbf{0} \end{bmatrix}, \tag{3}$$

Design Automation Conference ®

0-89791-847-9/97/0006/$3.50 DAC 97 - 06/97 Anaheim, CA, USA

by ordering the nodal voltages (type 1) before the branch currents (type 2). The subscript “1” represents type 1 matrices, “2” represents type 2 matrices, and “3” represents the connecting matrices between the type 1 and type 2 components. Here, $\mathbf{x_1}$ represents the nodal voltages of the system, and $\mathbf{x_2}$ represents the currents through the type 2 branches. The excitation vector $\mathbf{b_1}$ represents the currents injected into the nodes of the network, and by definition $\mathbf{b_2}$ is zero because the branch voltages of the type 2 elements cannot be externally excited. For simplicity, the time independent matrix, $\mathbf{G}$, is referred to as the conductance matrix even though all units are not conductance. In the same way, the time dependent matrix, $\mathbf{C}$, is referred to as the susceptance matrix.

It can be shown that if the RLC elements are positive and the magnitudes of the inductive coupling coefficients are less than or equal to one, the partitions of (3) have the following properties:

1) The type 1 conductance matrix, $\mathbf{G_1}$, is symmetric and nonnegative definite.
2) The type 1 susceptance matrix, $\mathbf{C_1}$, is symmetric and nonnegative definite.
3) The type 2 conductance matrix, $\mathbf{G_2}$, is symmetric nonpositive definite.
4) The type 2 susceptance matrix, $\mathbf{C_2}$, is symmetric nonpositive definite.
5) The susceptance matrix connecting type 1 and type 2 components, $\mathbf{C_3}$, is zero.
6) The type 2 excitation vector, $\mathbf{b_2}$, is zero, i.e. type 2 state variables are not excitable by the ports.

The term “symmetric nonnegative definite” denotes that no eigenvalue of the matrix is less than zero, and “symmetric nonpositive definite” indicates that no eigenvalue is greater than zero.

The six properties listed above form conditions which are sufficient for passivity, and thus these conditions are referred to as the “*passive form*” of the network. Theorem 1 shows than any RLC network which is in passive form is passive through the ports.

Theorem 1. Conditions sufficient for a network to be passive are:

1) The type 1 conductance and susceptance matrices are symmetric nonnegative definite.

2) The type 2 conductance and susceptance matrices are symmetric nonpositive definite.

3) The susceptance matrices which connect type 1 to type 2 elements is zero.

4) The type 2 ports are not excitable.

Proof: A partitioning of the MNA network matrices into type 1 and type 2 elements can be formed according (3). Because the second partition of $\mathbf{b}$ is zero, the second row of (3) can be multiplied by –1 without changing the voltage-current relationship at the type 1 network nodes to give

$$\left(\underbrace{\begin{bmatrix}\mathbf{G_1} & \mathbf{G_3^T}\\ -\mathbf{G_3} & -\mathbf{G_2}\end{bmatrix}}_{\tilde{\mathbf{G}}} + s\underbrace{\begin{bmatrix}\mathbf{C_1} & \mathbf{0}\\ \mathbf{0} & -\mathbf{C_2}\end{bmatrix}}_{\tilde{\mathbf{C}}}\right)\begin{bmatrix}\mathbf{x_1}\\ \mathbf{x_2}\end{bmatrix} = \begin{bmatrix}\mathbf{b_1}\\ \mathbf{0}\end{bmatrix}. \qquad (4)$$

The conditions for passivity are now applied to $\mathbf{W}(s) = \tilde{\mathbf{G}} + s\tilde{\mathbf{C}}$. From Wohlers [10], necessary and sufficient conditions for $\mathbf{W}(s)$ to be positive real (passive) are:

1) Each element of $\mathbf{W}(s)$ is analytic (no poles) for $\sigma > 0$.
2) $\mathbf{W}(s^*) = \mathbf{W}^*(s)$ where * is the complex conjugate operator.
3) $\mathbf{W}'(s) = \frac{1}{2}[\mathbf{W^T}(s^*) + \mathbf{W}(s)] = \mathbf{G} + \sigma\mathbf{C}$ is a nonnegative definite matrix for $\sigma > 0$.

Requirements 1 and 2 are always met because $w_{kl}(s) = g_{kl} + sc_{kl}$, and g_{kl} and c_{kl} are real scalars. To show requirement 3, let $s = \sigma + j\omega$ be complex frequency where σ and ω are real, and $j = \sqrt{-1}$. Because the diagonal blocks of both matrices are symmetric and the off diagonal blocks of the susceptance matrix are zero, one-half of the sum of $\mathbf{W}(s)$ and its complex transpose is:

$$\mathbf{W}'(s) = \begin{bmatrix}\mathbf{G_1} & \mathbf{0}\\ \mathbf{0} & -\mathbf{G_2}\end{bmatrix} + \sigma\begin{bmatrix}\mathbf{C_1} & \mathbf{0}\\ \mathbf{0} & -\mathbf{C_2}\end{bmatrix} \qquad (5)$$

If the type 1 blocks are nonnegative definite, the type two blocks are nonpositive definite, and $\sigma \geq 0$, then $\mathbf{W}'(s)$ is the sum of two symmetric nonnegative definite matrices, and such a sum is also symmetric nonnegative definite. All three requirements are met, and the network is passive.
QED.

---

3. Split Congruence Transformations

The passivity of reduced networks can be insured by preserving the passive form of the network throughout the reduction process. This section shows that a class of transformations, called “Split Congruence Transformations” (SCT’s), can be used to preserve the passive form. Congruence transformations can be used to reduce a network because they have the following form

$$\tilde{\mathbf{G}} + s\tilde{\mathbf{C}} = \mathbf{X^T G X} + s\mathbf{X^T C X}, \qquad (6)$$

and if the congruence transform, $\mathbf{X}$, has fewer columns then rows, then the transformed network is smaller than the original. A SCT has the form

$$\tilde{\mathbf{G}} = \mathbf{X^T G X} = \begin{bmatrix}\mathbf{X_1^T} & \mathbf{0}\\ \mathbf{0} & \mathbf{X_2^T}\end{bmatrix}\begin{bmatrix}\mathbf{G_1} & \mathbf{G_3^T}\\ \mathbf{G_3} & \mathbf{G_2}\end{bmatrix}\begin{bmatrix}\mathbf{X_1} & \mathbf{0}\\ \mathbf{0} & \mathbf{X_2}\end{bmatrix} \qquad (7)$$

and

$$\tilde{\mathbf{C}} = \mathbf{X^T C X} = \begin{bmatrix}\mathbf{X_1^T} & \mathbf{0}\\ \mathbf{0} & \mathbf{X_2^T}\end{bmatrix}\begin{bmatrix}\mathbf{C_1} & \mathbf{0}\\ \mathbf{0} & \mathbf{C_2}\end{bmatrix}\begin{bmatrix}\mathbf{X_1} & \mathbf{0}\\ \mathbf{0} & \mathbf{X_2}\end{bmatrix}, \qquad (8)$$

and it can be shown that this transformation preserves the passive form. The transform is called “split” because it is split into type 1 and type 2 blocks (i.e. there are no nonzero elements in the off diagonal blocks between the type 1 and type 2 partitions of the transform). The next section provides SCT’s which perform a number of different types of network reduction operations.

4. Network Reduction Using SCT’s

This section formulates the multiport admittance an RLC network, and shows how that network can be reduced. First, the MNA network matrices in (3) are partitioned into port and internal nodes so that the multiport admittance can be derived. A full rank SCT is then presented which can be used to zero the connection susceptance matrix, and a nonsquare SCT is given which reduces the size of the network while preserving some designated behavior. Finally, it is discussed that SCT’s can be used to remove DC singularities from the network. The SCT’s presented here are demonstrated in Section 5.

4.1 Formulation of the Multiport Admittance

Given an RLC network, which is represented using MNA by the matrices in (3), with m ports, n internal voltage nodes, and l type 2 elements, the multiport admittance can by found by partitioning the network into port nodes and internal nodes. The type 1 (voltage) nodes are ordered so that the common port node is 0, the remaining port nodes are in the first m rows, and the n internal voltage nodes are in the next n rows. The type 1 matrices are then partitioned as

$$\left(\begin{bmatrix} \mathbf{G_P} & \mathbf{G_{C1}^T} & \mathbf{G_{C2}^T} \\ \mathbf{G_{C1}} & \mathbf{G_{I1}} & \mathbf{G_{I3}^T} \\ \mathbf{G_{C2}} & \mathbf{G_{I3}} & \mathbf{G_2} \end{bmatrix} + s\begin{bmatrix} \mathbf{C_P} & \mathbf{C_{C1}^T} & \mathbf{0} \\ \mathbf{C_{C1}} & \mathbf{C_{I1}} & \mathbf{0} \\ \mathbf{0} & \mathbf{0} & \mathbf{C_2} \end{bmatrix}\right)\begin{bmatrix} \mathbf{x_P} \\ \mathbf{x_{I1}} \\ \mathbf{x_2} \end{bmatrix} = \begin{bmatrix} \mathbf{b_P} \\ \mathbf{0} \\ \mathbf{0} \end{bmatrix}. \tag{9}$$

The m port node voltages are represented by $\mathbf{x_P}$, the n internal node voltages are represented by $\mathbf{x_{I1}}$, and the l branch currents are represented by $\mathbf{x_2}$. The currents injected into the m ports are given by $\mathbf{b_P}$. The type 1 internal excitation vector is zero because no current can be injected into an internal node, and the type 2 excitation vector is zero by definition. The $m \times m$ port conductance and susceptance matrices are given by $\mathbf{G_P}$ and $\mathbf{C_P}$ respectively, and the $(l+n) \times m$ connection conductance and susceptance matrices are given by

$$\mathbf{G_C} = \begin{bmatrix} \mathbf{G_{C1}} \\ \mathbf{G_{C2}} \end{bmatrix} \text{ and } \mathbf{C_C} = \begin{bmatrix} \mathbf{C_{C1}} \\ \mathbf{0} \end{bmatrix}. \tag{10}$$

Finally, the $(l+n) \times (l+n)$ internal conductance and susceptance matrices are

$$\mathbf{G_I} = \begin{bmatrix} \mathbf{G_{I1}} & \mathbf{G_{I3}^T} \\ \mathbf{G_{I3}} & \mathbf{G_2} \end{bmatrix} \text{ and } \mathbf{C_I} = \begin{bmatrix} \mathbf{C_{I1}} & \mathbf{0} \\ \mathbf{0} & \mathbf{C_2} \end{bmatrix}. \tag{11}$$

To formulate the multiport admittance, $\mathbf{Y}(s)$, (9) is simplified by using the identities given in (10) and (11).

$$\left(\begin{bmatrix} \mathbf{G_P} & \mathbf{G_C}^{\mathbf{T}} \\ \mathbf{G_C} & \mathbf{G_I} \end{bmatrix} + s\begin{bmatrix} \mathbf{C_P} & \mathbf{C_C}^{\mathbf{T}} \\ \mathbf{C_C} & \mathbf{C_I} \end{bmatrix}\right)\begin{bmatrix} \mathbf{x_P} \\ \mathbf{x_I} \end{bmatrix} = \begin{bmatrix} \mathbf{b_P} \\ \mathbf{0} \end{bmatrix}. \tag{12}$$

Equation (12) provides two equations with two unknowns, $\mathbf{x_P}$ and $\mathbf{x_I}$. Using the definition

$$\mathbf{Y}(s)\,\mathbf{x_P}(s) = \mathbf{b_P}(s) \tag{13}$$

and eliminating $\mathbf{x_I}$ gives

$$\mathbf{Y}(s) = \mathbf{G_P} + s\mathbf{C_P} - (\mathbf{G_C} + s\mathbf{C_C})^{\mathbf{T}}(\mathbf{G_I} + s\mathbf{C_I})^{-1}(\mathbf{G_C} + s\mathbf{C_C}) \tag{14}$$

The poles of $\mathbf{Y}(s)$ occur where $(\mathbf{G_I} + s\mathbf{C_I})$ is singular, and these are found from the solution to the generalized eigenvalue problem

$$\mathbf{G_I x} = \lambda \mathbf{C_I x} \tag{15}$$

where $s = -\lambda$ is a pole of the system.

4.2 Zeroing the Connection Susceptance Matrix

It is desirable to simplify (14) by zeroing $\mathbf{C_C}$ without changing the network behavior. The primary benefit of this is that the span requirements, which are presented in the next subsection, are simplified. A second benefit is that the branch count of the reduced network is decreased.

Application of the split congruence transform

$$\mathbf{X} = \left[\begin{array}{cc:c} \mathbf{I} & \mathbf{0} & \mathbf{0} \\ -\mathbf{C_{I1}^{-1}C_{C1}} & \mathbf{I} & \mathbf{0} \\ \hdashline \mathbf{0} & \mathbf{0} & \mathbf{I} \end{array}\right] \tag{16}$$

to the RLC network matrices given in (9) causes the susceptance connection matrix to be zero as illustrated in (17) and (18). The dotted lines separate the type 1 (upper left) and type 2 (low right) partitions of the transform to illustrated that it is a SCT.

$$\tilde{\mathbf{G}} = \mathbf{X^T G X} = \begin{bmatrix} \tilde{\mathbf{G}}_{\mathbf{P}} & \tilde{\mathbf{G}}_{\mathbf{C1}}^{\mathbf{T}} & \tilde{\mathbf{G}}_{\mathbf{C2}}^{\mathbf{T}} \\ \tilde{\mathbf{G}}_{\mathbf{C1}} & \mathbf{G_{I1}} & \mathbf{G_{I3}^T} \\ \tilde{\mathbf{G}}_{\mathbf{C2}} & \mathbf{G_{I3}} & \mathbf{G_2} \end{bmatrix} \tag{17}$$

and

$$\tilde{\mathbf{C}} = \mathbf{X^T C X} = \begin{bmatrix} \tilde{\mathbf{C}}_{\mathbf{P}} & \mathbf{0} & \mathbf{0} \\ \mathbf{0} & \mathbf{C_{I1}} & \mathbf{0} \\ \mathbf{0} & \mathbf{0} & \mathbf{C_2} \end{bmatrix}, \tag{18}$$

and a straightforward substitution of the partitions of $\tilde{\mathbf{G}}$ and $\tilde{\mathbf{C}}$ into (14) shows that the multiport admittance, $\mathbf{Y}(s)$, is unchanged. It is shown in [11] that, even if $\mathbf{C_{I1}}$ is singular, a SCT always exists which will zero the connection susceptance matrix if the original network is in passive form.

4.3 Preservation of Admittance Poles and Moments

A network represented by (9) can be reduced in size by application of a SCT of the form

$$\mathbf{X} = \left[\begin{array}{cc:c} \mathbf{I} & \mathbf{0} & \mathbf{0} \\ \mathbf{0} & \mathbf{V_1} & \mathbf{0} \\ \hdashline \mathbf{0} & \mathbf{0} & \mathbf{V_2} \end{array}\right] \tag{19}$$

so that

$$\tilde{\mathbf{G}} = \mathbf{X^T G X} = \begin{bmatrix} \mathbf{G_P} & \mathbf{G_{C1}^T V_1} & \mathbf{G_{C2}^T V_2} \\ \mathbf{V_1^T G_{C1}} & \mathbf{V_1^T G_{I1} V_1} & \mathbf{V_1^T G_{I3}^T V_2} \\ \mathbf{V_2^T G_{C2}} & \mathbf{V_2^T G_{I3} V_1} & \mathbf{V_2^T G_2 V_2} \end{bmatrix} \tag{20}$$

and the same is done for the partitions of $\mathbf{C}$. Substitutions of the transformed network into the formulation of the multiport admittance in (14) shows that it is unchanged when $\mathbf{V}_1$ and $\mathbf{V}_2$ are square and nonsingular. The size of the network is reduced when the partitions of $\mathbf{V}$ have fewer columns than rows, but this transform no longer preserves all of the network behavior. Fortunately, it is possible to preserve poles and moments of the multiport admittance is as shown in the next two paragraphs.

Poles are preserved if the SCT spans the eigenvectors associated with the admittance poles of the original network. Given the complex vector $\mathbf{x}$ from (15) which is associated with a particular pole of $\mathbf{Y}(s)$, it is shown in [11] that if

$$\mathrm{span}(\mathbf{x}) \subseteq \mathrm{span}(\mathbf{V}) \tag{21}$$

where

$$\mathbf{V} = \begin{bmatrix} \mathbf{V_1} & \mathbf{0} \\ \mathbf{0} & \mathbf{V_2} \end{bmatrix} \tag{22}$$

is the internal partition of the real transform in (19), then the reduced network will retain that pole. Equation (21) simply implies that some linear combination of the columns of $\mathbf{V}$ can be used to form the vector $\mathbf{x}$, and this is useful if it is desired to exactly retain a particular set of poles, such as those which lie on the imaginary axis. The eigenvectors associated with a the desired poles can be calculated using a sparse or dense eigenanalysis technique, and the transform given in (19) is built by setting the type 1 and type 2 portions of $\mathbf{V}$ to the type 1 and type 2 portions of the eigenvectors. A technique such as modified Gram-Schmidt orthogonalization should be used to make sure that the columns of $\mathbf{V}$ are real and linearly independent.

Moments of the Taylor series expansion of $\mathbf{Y}(s)$ about a frequency $s = s_0$ can be preserved in a manner similar to that used to preserve the poles. It is shown in [11] that if the connection susceptance matrix, $\mathbf{C_C}$, is zero, then the first $2q$ moments of the multiport admittance are preserved when the columns of $\mathbf{V}$ in (22) span the Krylov subspace

$$\mathbf{K}_q\left(\mathbf{A}^{-1}\mathbf{C_I}, \mathbf{A}^{-1}\mathbf{G_C}\right) = \mathrm{span}(\tilde{\mathbf{V}}) \tag{23}$$

where

$$\mathbf{A} = \mathbf{G_I} + s_0\mathbf{C_I}. \tag{24}$$

This span requirement is similar to that derived for MPVL and the Arnoldi-based method. One difference, however, is that since both the Arnoldi and Lanczos methods form a matrix $\tilde{\mathbf{V}}$ with the span requirements given by (23), *either* method can be used to generate a transform which preserves $2q$ moments. In contrast, the Arnoldi-based method presented in [7] only preserves half as many moments. To form a SCT, the type 1 and type 2 portions of $\mathbf{V}$ are formed from the corresponding parts of $\tilde{\mathbf{V}}$, and the columns are made linearly independent. The SCT does not form a Padé approximation because splitting $\tilde{\mathbf{V}}$ into two separate blocks generally increases the number of internal nodes in the reduced network — $2q$ moments are matched, but there are more than qm internal nodes (m is the number of ports).

Finally, it is possible to mix the different span requirements into the same SCT. For instance, a well conditioned SCT can be built which preserves a pole a 1 GHz, the first 6 moments expanded at DC, and the first 4 moments expanded at f = 500 MHz. Each individual set of spans are calculated using eigenanalysis and Krylov subspace algorithms, and then are split into type 1 and type 2 blocks to form the transform. Again, a technique such as modified Gram-Schmidt orthogonalization should be used to ensure the columns of the transform are linearly independent.

4.4 Elimination of DC Singularities

Networks which have floating nodes or current loops have a valid solution to the multiport admittance at the ports, but the internal conductance matrix, $\mathbf{G_I}$, is singular. Floating nodes cause a singularity because there is no DC path to these nodes, so that they can support a nonzero voltage even when the input current is zero. When inductors form a loop, a singularity is created because a DC current can be sustained through the loop even when all voltages are zero.

It is possible to form a SCT which separates the DC singularities from the remaining nonsingular network. The nonsingular part of the network is in passive form and has the same partitions shown in (9). The singular network has the form

$$\mathbf{G}' = \begin{bmatrix} \mathbf{0} & \mathbf{G_C}'^{\mathbf{T}} \\ \mathbf{G_C}' & \mathbf{0} \end{bmatrix} \text{ and } \mathbf{C}' = \begin{bmatrix} \mathbf{0} & \mathbf{0} \\ \mathbf{0} & \mathbf{C_I}' \end{bmatrix}, \tag{25}$$

and the singular and nonsingular networks are added in parallel at the ports. If a DC pole is seen by the ports then $\mathbf{G_C}'$ is nonzero, and it is important to extract the port poles from (25) and include them with the final reduced network in order to preserve the dc behavior. Sparse techniques can be employed by avoiding explicit formulations of the singular and nonsingular network matrices, and an example of this is given in Section 5.2.

5. Examples of SCT-based Network Reduction

Several examples of examples of RLC network reduction are provided which employ the SCT's introduced in the previous section. A general RLC network is reduced in Section 5.1 which illustrates the while Padé approximations can result in unstable networks, SCT-derived networks preserve asymptotic stability. Section 5.2 shows the sparse reduction of an industry network using a prototype reduction tool based on SCT's. All simulations are performed using HSPICE [12] on a SUN SPARC 20 workstation, and network reduction in the first example is implemented in MATLAB [8].

Table 1. Statistics for RLC test network.

Ports	Internal Nodes	Resistors	Capacitors	Inductors	Mutual Inductors
2	159 (41 voltage)	38	38	118	524

5.1 Network Reduction Using DC Moment Matching

This section shows the reduction of a general RLC network by matching moments at DC, and demonstrates that SCT's preserve asymptotic stability while providing accuracy which is comparable to the non-split techniques. A random two-port RLC test network is used which contains all passive elements, and the number of elements contained in the network is given in Table 1. The network has 79 singularities at DC, two of which are seen through the ports. The first step in the reduction is to eliminate the DC singularities by using the transform discussed in Section 4.4. Next, the susceptance connection matrix is zeroed using the transform given in Section 4.2, and the span given by (23) to preserve the DC moments is calculated using the Arnoldi process.

Two separate reductions are performed. The first uses the transform without splitting, and this is a Padé approximation because two moments are matched per m internal nodes, where m = 2 is the number of ports. The second reduction splits the transform so that passivity is preserved, and, as a result, only one moment per m internal nodes is preserved. For this example, two additional internal nodes in the reduced networks are required to preserve the DC poles seen through the ports.

Table 2 provides the statistics on the reduced networks used in this example. The SCT networks match half as many moments as do the Padé networks of the same size. On the other hand, SCT reduced networks *never* have unstable poles (i.e. poles whose real part is greater than zero) because asymptotic stability is a requirement of passivity and passivity is *always* preserved. In this example, the Padé network reduction creates some unstable poles which make the reduced network useless for transient circuit simulation. Once enough moments are preserved that the reduced network behaves like the original over the entire frequency range, these poles disappear (e.g. 60 moments matched in this example).

The number of elements in the reduced network increases as the square of the number of internal nodes because the reduced matrices are dense, and this is shown in the second column from the right in the table. This superlinearity can be eliminated by applying a non-split, well conditioned square congruence transform which block diagonalizes the internal conductance matrix and diagonalizes the internal susceptance matrix. In the resulting network, the element count increases linearly with the number of nodes, and, although it is not in passive form, passivity is preserved because the transform exactly preserves the reduced net-

Table 2. Statistics for RLC network reduction

	Moments Matched	Internal Nodes	Unstable Poles	Elements (no diagonalizing)	Elements (diagonalizing)
SCT	10	22	0	330	102
	20	42	0	1145	191
	30	62	0	2460	279
Padé	20	22	**2**	475	102
	40	42	**2**	1735	192
	60	62	0	3795	280

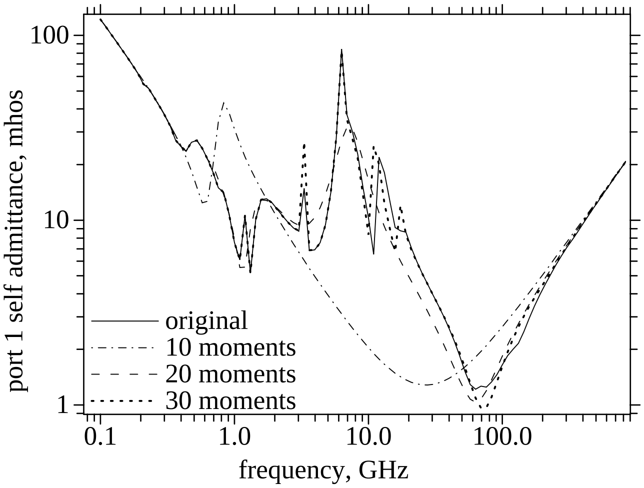

Figure 1. Port 1 self admittance of the original and SCT reduced networks given in Tables 1 and 2.

work's behavior. The right-most column of the table shows the element count after the networks are block diagonalized.

The accuracy of the reductions can be seen in Figures 1 and 2 which show that the fit improves as the number of matched moments is increased. The behavior of the network is almost completely matched over the entire frequency range when 30 moments are matched using the SCT's or 60 moments are matched using Padé approximations. The Padé networks are somewhat more accurate for the same number of internal nodes since they match more moments, but the increase in accuracy versus network size is at the expense of creating reduced networks which are unstable. If the two techniques are compared versus the number of moments matched (e.g. 20 moments in this example) instead of reduced network size, the SCT networks are more accurate.

5.2 Sparse RLC Reduction

This final example demonstrates the sparse implementation of the SCT's in a prototype network reduction tool which is passed a network and a frequency range and error tolerance for which accuracy must be preserved. The tool is created to demonstrate the sparse implementation of the SCT's presented in Section 4 and is not being proposed as an ideal implementation which is suitable for industry. Sparse matrix inversions are performed by Sparse

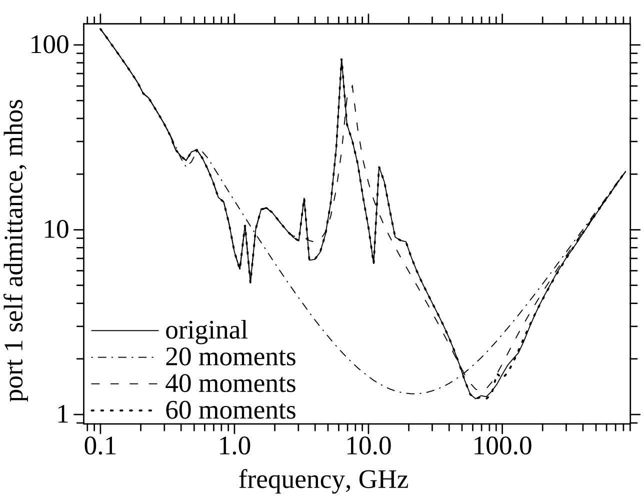

Figure 2. Port 1 self admittance of the original and Padé approximation networks given in Tables 1 and 2.

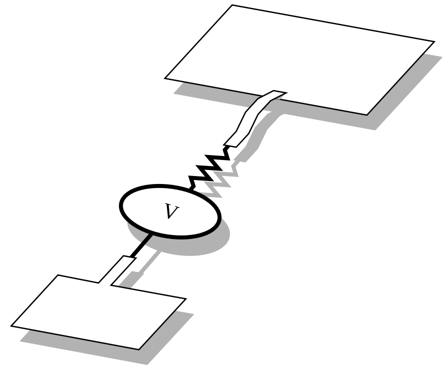

Figure 3. Topology of PEEC model and driving circuit.

[13], and dense linear algebra functions such as eigendecomposition and matrix inversion are performed by LAPACK [14].

The basic operation of the tool is as follows. First, a SPICE netlist is parsed, the RLC and K branch elements are extracted, and the port nodes are identified. DC singularities are handled as described in Section 4.4. Next, poles in the frequency range of interest which lie on the imaginary axis are identified using a technique similar to CFH — this has the same disadvantage of CFH, i.e. multiple complex LU factorizations need to be performed, but it works well for demonstration purposes since it allows different types of span requirements (eigenvectors as well as moments expanded at different frequencies) to be calculated and combined in a single SCT. The eigenvectors associated with complex poles are found and are added to the SCT matrix which is used to reduce the network. The span required to preserve the first two moments at DC is found using (23), and this is split and added to the SCT matrix as well. A series of hops are then taken at frequencies on the imaginary axis, and, if the error in the reduced network exceeds the error tolerance at the hop's frequency, then some or all of the span required to match the first two moments at that frequency is added to the SCT matrix. The additional span causes the relative error to drop below the specified error tolerance at that frequency since the slope and offset of the reduced network are identical to the original when the entire span is added to the transform. The process is continued until the error of the reduced network is less than the error tolerance over the entire frequency range. The final step of the reduction is to block diagonalize the reduced network matrix.

In this example, the network to be reduced is a PEEC model [1] with a topology similar to that shown in Fig. 3. Two lossless metal plates or lines are floating over a ground plane. The plates are modeled using an inductor mesh containing 42 closed loops (DC singularities), and these are coupled via mutual inductance and capacitance. In addition, the mesh voltage nodes have capacitance to ground. The two-port network is driven by a Thevenin voltage source for simulation, and a 100 MΩ resistor is added between one of the voltage node terminals and ground. The number of elements in the original model is given in Table 1. The inductors are given a resistance of 10^{-15} Ω for the HSPICE simulations so that the simulator does not fail due to singularities encountered during the DC operating point calculation.

The network is reduced twice. The first reduction is performed on the LC elements only (LC reduction) with a specified accuracy

Table 3. Network statistics for PEEC model.

Ports	Internal Nodes	Resistors	Capacitors	Inductors	Mutual Inductors
2	302 (130 voltage)	0	2100	172	6990

Table 4. PEEC model reduction and simulation results.

Network	Internal Nodes	Element count	Reduction		Simulation	
			CPU sec	MByte	CPU sec	MByte
original	302	9264	—	—	753.9	10.2
LC	15	59	93.2	2.8	0.2	0.2
RLC	14	75	91.7	3.4	0.2	0.2

of 5% between DC and 1 GHz. The second is performed on the network which also includes the Thevenin resistance (RLC reduction). The tool predominantly uses a pole analysis in the first case since the poles are on the complex axis, and it uses moment expansions at multiple frequencies in the second case. The statistics on the network reductions and HSPICE simulations are given in Table 4. The reductions take an order of magnitude less time than the simulations and speed the simulations by several orders of magnitude. The HSPICE simulations are AC frequency sweeps of the voltage source, and the output is the current through the voltage source. The results of these simulations are given in Fig. 4, and it can be seen that for both cases, the reduced networks are accurate over the specified frequency range.

6. Concluding Remarks

The main concept presented in this paper is that the MNA matrices which represent positive RLC networks have a passive form, and network reduction based on split congruence transformations (SCT's) preserves the passive form and thus ensures that the reduced networks remain passive. It is shown that SCT's can be used to provide well conditioned admittance-to-admittance transformations of a general RLC network which preserve selected poles or moments of the network multiport admittance while reducing the size of the network. All congruence transforms of RC networks and those which preserve poles and moments of LC networks are naturally split, and therefore always preserve passivity. The several examples of reduction using SCT's demonstrate the stability of the SCT-derived networks and show that a sparse implementation using these transformations can be achieved.

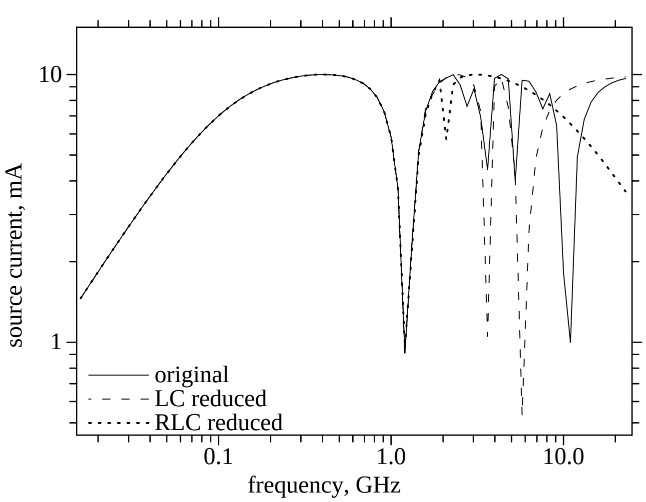

Figure 4. AC sweep to measure current through the voltage source as a function of frequency.

References

[1] A. E. Ruehli. "Equivalent circuit models for three dimensional multiconductor systems," *IEEE Trans. Microwave Theory and Technique*, MTT-22(3), pp. 216-221, March 1974.

[2] K. Kamon, M. J. Tsuk, and J. White, "Fasthenry, a multipole-accelerated 3-d inductance extraction program," *Proceedings of the 30th ACM/IEEE Design Automation Conference*, pp. 678-683, June 1993.

[3] I. L. Wemple and A. T. Yang, "Integrated circuit substrate coupling models based on Voronoi tessellation," *IEEE Trans. Computer-Aided Design*, vol. 14, pp. 1459-1469, December 1995.

[4] L. T. Pillage and R. A. Rohrer, "Asymptotic waveform evaluation for timing analysis," *IEEE Trans. Computer-Aided Design*, vol. 9, pp. 352-366, April 1990.

[5] E. Chiprout and M. S. Nakhla, "Analysis of interconnect networks using complex frequency hopping (CFH)," *IEEE Trans. Computer-Aided Design*, vol. 14, pp.186-200, February 1995.

[6] P. Feldmann and R. W. Freund, "Reduced-order modeling of large linear subcircuits via a block Lanczos algorithm," *Proceedings of the 32nd ACM/IEEE Design Automation Conference*, pp. 474-479, June 1995.

[7] L. M. Silveira, M. Kamon, and J. White, "Efficient reduced-order modeling of frequency-dependent coupling inductances associated with 3-D interconnect structures," *Proceedings of the 32nd ACM/IEEE Design Automation Conference*, pp. 376-380, June 1995.

[8] MATLAB, The MathWorks, Inc., Version 4.2, Natick, MA.

[9] C.-W. Ho, A. E. Ruehli and P. A. Brennan, "The modified nodal approach to network analysis," *IEEE Trans. Circuits and Systems.*, vol. CAS-22, pp. 504-509, June 1975.

[10] M. R. Wohlers, *Lumped and Distributed Passive Networks: A Generalized and Advanced Viewpoint*. New York: Academic Press, 1969.

[11] K. J. Kerns, *Accurate and Stable Reduction of RLC Networks Using Split Congruence Transformations*. Ph.D. dissertation. University of Washington, Seattle, WA, September, 1996.

[12] HSPICE, Meta-Software, Inc., Version H95.1, Campbell, CA, 1995.

[13] K. S. Kundert and A. Sangiovanni-Vincentelli, *User's Guide for Sparse: A Sparse Linear Equation Solver.* Version 1.3a, Department of EECS, University of California, Berkeley, CA, 1988.

[14] E. Anderson, *et al. LAPACK User's Guide*, 2nd edition, Philadelphia: Society for Industrial and Applied Mathematics, 1995.